

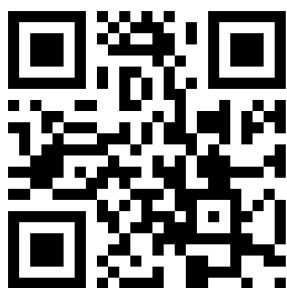
The Optimization Design Of Lactoferrin Loaded HupA Nanoemulsion For Targeted Drug Transport Via Intranasal Route

This article was published in the following Dove Press journal:
International Journal of Nanomedicine

Yueyao Jiang
Chenqi Liu
Wanchen Zhai
Ning Zhuang
Tengfei Han 
Zhiying Ding

School of Pharmaceutical Sciences, Jilin University, Changchun 130021, People's Republic of China

→ Video abstract



Point your SmartPhone at the code above. If you have a QR code reader the video abstract will appear. Or use:
<https://youtu.be/EpqKwDyguVs>

Background: Huperzine A (HupA) is a selective acetylcholinesterase inhibitor used to treat Alzheimer's disease. The existing dosage of HupA lacks brain selectivity and can cause serious side effects in the gastrointestinal and peripheral cholinergic systems.

Purpose: The aim of this study was to develop and characterize a HupA nanoemulsion (NE) and a targeted HupA-NE modified with lactoferrin (Lf) for intranasal administration.

Methods: The NE was formulated using pseudo-ternary phase diagrams and optimized with response surface methodology. Particle size distribution and zeta potential were evaluated, and transmission electron microscopy was performed. We investigated the transport mechanisms of HupA-NEs into hCMEC/D3 cells, an in vitro model of the blood-brain barrier. HupA-NE, Lf-HupA-NE, and HupA solution were intranasally administered to rats to investigate the brain-targeting effects of these formulations. A drug targeting index (DTI) was calculated to determine brain-targeting efficiency.

Results: Optimized HupA-NE had a particle size of 15.24 ± 0.67 nm, polydispersity index (PDI) of 0.128 ± 0.025 , and zeta potential of -4.48 ± 0.97 mV. The composition of the optimized HupA-NE was 3.00% isopropyl myristate (IPM), 3.81% Capryol 90, and 40% Cremophor EL + Labrasol. NEs, particularly Lf-HupA-NE, were taken up into hCMEC/D3 cells to a greater extent than pure drug alone. Western blot analysis showed that hCMEC/D3 cells contained P-glycoprotein (P-gp), breast cancer resistance protein (BCRP), and multidrug resistance associated protein 1 (MRP1) transporters. The likely mechanisms resulting in higher NE transport to the brain were uptake by specific transporters and transcytosis. In vivo, intranasal Lf-HupA-NE significantly enhanced drug delivery to the brain compared to HupA-NE, which was confirmed by differences in pharmacokinetic parameters. The DTI of Lf-HupA-NE (3.2 ± 0.75) demonstrated brain targeting, and the area under the curve for Lf-HupA-NE was significantly higher than that for HupA-NE.

Conclusion: Lf-HupA-NE is a promising nasal drug delivery carrier for facilitating delivery of HupA to the central nervous system.

Keywords: nanoemulsion, lactoferrin, brain targeting, intranasal delivery

Introduction

Alzheimer's disease (AD) is the leading cause of age-related dementia, and its incidence is increasing dramatically due to longer lifespans and a growing aging population.¹ The early stage of AD is characterized by short-term memory loss, eventually followed by disorientation, agitation, psychosis, and death due to loss of bodily functions.² Huperzine A (HupA), a reversible acetylcholinesterase inhibitor (AChEI), enhances memory in behavioral animal models and also exerts multiple neuroprotective effects.³ However, only oral and injectable preparations of HupA are

Correspondence: Zhiying Ding
School of Pharmaceutical Sciences, Jilin University, Changchun 130021, People's Republic of China
Tel +8613843180286
Email dzy@jlu.edu.cn

available, and these formulations lack brain selectivity, resulting in gastrointestinal side effects such as nausea and vomiting, which are characteristic of AChEIs. These side effects increase the likelihood of discontinuing treatment.⁴ Furthermore, injectable HupA is painful for patients, difficult to administer at home, or need a highly harsh medical conditions for the injection. A novel drug delivery system is needed to improve transport and distribution of HupA to the brain. Nanoemulsions (NEs) prepared as an isotropic mixture of oil, water, and surfactant/cosurfactant are commonly used for drug delivery as these formulations are clear and thermodynamically stable.^{5,6} Drugs formulated in NEs can have enhanced pharmacokinetics and pharmacodynamics, as evidenced by greater extended-release properties and prolonged pharmacological efficacy. NEs have also been shown to mitigate toxicity and side effects.⁷ Since the goal of nanomedicines is to offer controlled release of drugs into disease sites,⁸ NEs have received increasing attention.

Recently, focus has shifted to the intranasal route as a non-invasive alternative to deliver therapeutics because this route can deliver drugs directly to the brain,⁹ bypassing gastrointestinal and hepatic first pass metabolism.¹⁰

Lactoferrin (Lf) is a natural iron-binding cationic glycoprotein (MW 80 kDa). This member of the transferrin family is expressed in various tissues and involved in many physiological processes.¹¹ Previous studies showed high Lf receptor expression in respiratory epithelial cells,¹² brain endothelial cells and neurons. They are particularly over-expressed in the central nervous systems (CNS) of individuals with age-related neurodegenerative diseases.¹³ Therefore, we hypothesized that Lf-modified NE might exhibit enhanced brain-targeted delivery of HupA via the intranasal route.

The aim of this study was to prepare HupA-NE and Lf-HupA-NE for intranasal delivery to the brain for treatment of AD. In vivo pharmacokinetic profiles and drug targeting indexes (DTIs) of HupA-NE and Lf-HupA-NE were evaluated. Finally, we used an in vitro blood-brain barrier (BBB) model (hCMEC/D3 cells) to determine how NEs access the brain parenchyma.

Materials And Methods

Materials

HupA was supplied by MULTI SCIENCES (Hangzhou, China). Lactoferrin was bought from Yuanye Biological Technology Co., Ltd (Shanghai, China). Rhodamine B (RhB) was procured from Adamas-beta (Shanghai, China). Propylene glycol monocaprylate (Capryol 90), Oleoyl

polyoxyl-6 glycerides (LABRAFIL[®] M 1944 CS), Polyglyceryl-3 dioleate (Plurol[®] Oleique CC 497) and Caprylocaproyl Macrogolglycerides (Labrasol) were purchased from Gattefossé (Saint-Priest, France). IPM, 1-(3-Dimethylaminopropyl)-3-ethylcarbodiimide Hydrochloride (EDCI), 1-Hydroxybenzotriazole (HOBT) and N,N-Diisopropylethylamine (DIEA) were provided by Sinopharm Chemical Reagent Co.,Ltd (Shanghai, China). Tween 80 and Span 80 were obtained from Huadong Reagent Factory (Tianjin, China). Linear Alkylbenzene Sulfonates (L.A.S) was purchased from Enpu Biochemical Technology Co. Ltd (Shanghai China). All other solvents used were of analytical grade. The cell culture RPMI1640 media was from Gibco, Thermo Fisher Scientific. Dimethyl sulfoxide (DMSO), phosphate buffered saline (PBS), Triton x-100 were purchased from Absin Bioscience Inc. Endocytosis inhibitors, Genistein, colchicine, MK571, ko143, Amantadine were purchased from MedChemexpress, New Jersey, US. Chlorpromazine was manufactured by Solarbio. Verapamil, Aprotinin were purchased from Sigma-Aldrich. Anti-P Glycoprotein antibody [EPR10364] (ab168337), Anti-BCRP/ABCG2 antibody [EPR20080] (ab207732), Anti-MRP1 antibody [EPR21062] (ab233383), Anti-Oct-1 antibody [EPR16570] (ab178869), goat anti-rabbit IgG (H+L)-HRP (ab181448) secondary antibody were purchased from Abcam, Cambridge, UK.

4', 6'-diamidino-2-phenylindole (DAPI) was purchased from Molecular Probes (Eugene, OR, USA). Human cerebral microvascular endothelial cells, D3 clone (hCMEC/D3) cells were purchased by the American Type Culture Collection (ATCC, Beijing, China).

HPLC And Analytical Method

A C18 Columns (COSMOSIL PACKRD 5C18-MS-11, SHIMADZU, Japan) was utilized for drug separation, using methanol-water (43:57) as mobile phase. 1 mL triethanolamine was added 1000 mL water until pH=7. The flow rate was 1 mL/min and the retention time was 15.6 min. The detection was performed at 308 nm. The assays were performed at ambient temperature.

Preparation And Formulation Optimization Of HupA-Loaded NEs

Solubility Studies

HupA solubility was investigated in oils such as soybean oil, isopropyl myristate (IPM), L.A.S., Capryol 90, LABRAFIL[®] M 1944 CS, and olive oil. Surfactants and co-surfactants including Span 80, Cremophor EL, Labrasol, Tween 80, Plurol[®] Oleique CC 497, polyethylene glycol

(PEG) 400, and ethanol were also evaluated. The purpose was to identify solvents that were harmless to humans, had stable chemical properties, and did not react with HupA.

An excess amount of HupA was added to vials containing 0.2 mL of the vehicles. After sealing, the mixtures were continuously stirred using a vortex mixer for 10 min and kept at 37 ± 0.5 °C in a water bath shaker for 24 h to facilitate solubilization and proper mixing of the drug with the vehicles (Dragon Laboratory Instruments Limited, Beijing, China). The mixtures were then centrifuged at 6000 rpm for 10 min (Anke, Shanghai, China). The supernatants were filtered through 0.45 μ m membrane filters, 0.1 mL of supernatant from each tube was diluted with methanol, and the concentration of dissolved drug was determined using high-performance liquid chromatography (HPLC, SHIMADZU, Kyoto, Japan).

Pseudo-Ternary Phase Diagram Construction

Pseudo-ternary phase diagrams were constructed using the aqueous titration method to determine the region in which NEs would form and evaluate NE formation with different compositions of surfactant, co-surfactant, oil, and water. The surfactant and co-surfactant in each group were mixed (Smix) at different volume ratios (1:2, 1:1, 2:1). For each phase diagram, oil and the surfactant mixtures (S/CoS) were prepared in different combinations from 1:9 to 9:1. The NE phase was identified based on clarity and flowability. The percentage of each component was recorded to complete the pseudo-ternary phase diagrams.

Software Optimization Of NE Formulation

Based on initial screening, Cremophor EL, Labrasol, IPM, and Capryol 90 were chosen as components to form NE, and Smix was set at 2:1. To optimize HupA NE, we used a Box-Behnken design (BBD) that contained 3 factors, 3 levels, and 15 experimental runs to allow for optimization using Design-Expert Software (Design-Expert 8.0.6, Stat-Ease, Minneapolis, MN, USA). The independent variables with their low (-1), medium (0), and high levels (+1)¹⁴ and dependent variables are listed in Table 2. The concentration ranges of the independent variables were as follows: IPM (3–7%), Capryol 90 (3–7%), and S+CoS (30–40%). Each formulation was evaluated for particle size and polydispersity index (PDI).

Preparation Of HupA-NE And Lf-HupA-NE

HupA-NE was prepared in the solvents determined by the generated phase diagrams, and the optimal NE formulation

was determined using BBD. Based on the formulation optimization procedures, HupA was dissolved in the designated mixture of oil phase, Cremophor EL, and Labrasol. Then, water was added to the mixture drop by drop with constant stirring using a magnetic stirrer at ambient temperature. The final drug concentration of the NE was 5 mg/mL.

Lf dissolved in the water phase was slowly dropwise added to the mixture of oil and smix using a magnetic stirrer at ambient temperature to obtain Lf-HupA-NE. To avoid surface-active impurities, double-distilled water was used for HupA-NE and Lf-HupA-NE preparation.

RhB-HupA-NE And Lf-RhB-HupA-NE

HOBt (1.13 mmol) and EDCI (0.251 g, 1.13 mmol) were stirred into a solution of RhB (1.00 mmol) in CH_2Cl_2 (10.00 mL) at room temperature (RT) for 10 min, then DIEA (2.00 mmol) was added, and the mixture was stirred at RT. After 4 h, 1 mmol of HupA was added to the mixture. The resulting mixture was stirred at RT overnight. The reaction mixture was partitioned between ethyl acetate and H_2O . The organic layer was washed with H_2O , dried over MgSO_4 , and concentrated under reduced pressure. Following solvent evaporation, the residue was purified by silica gel chromatography ($\text{CH}_2\text{Cl}_2/\text{MeOH}$) to yield RhB-HupA. The product was characterized by infrared (IR) spectrum analysis (Thermo Fisher Scientific, Waltham, MA, USA). RhB-HupA was dissolved in the oil phase. RhB-HupA-NE and Lf-RhB-HupA-NE were obtained by the same procedure as NEs.

NE Characterization

Globule Size Analysis And Zeta Potential Measurement

Approximately 0.1 mL of NE and Lf-NE formulations were diluted in 50 mL of distilled water. Globule size and PDI were measured using dynamic light scattering (Nano-ZS90, Malvern Panalytic, Malvern, UK). Zeta potential was measured by photon correlation spectroscopy using a Zetasizer (Nano-ZS90). All measurements were performed at 25 °C in triplicate.¹⁵

Transmission Electron Microscopy Analysis

Transmission electron microscopy (TEM, Hitachi, Tokyo, Japan) analysis was performed to determine NE morphology. A drop each of diluted HupA-NE and Lf-HupA-NE was applied to a 300-mesh copper grid and stained with 2% (w/v) phosphotungstic acid (PTA) for 5 min. Excess PTA was removed using a piece of filter paper and dried at RT. The samples were analyzed by TEM.

Stability Study

To study physical stability, HupA-NE and Lf-HupA-NE were stored for 6 months at ambient RT. HupA-NE and Lf-HupA-NE were checked visually for drug sedimentation (creaming, flocculation, or phase separation), and analyzed for globule size, PDI, and zeta potential.

Drug Release Study

In vitro release of HupA from HupA-NE and Lf-HupA-NE were evaluated using a dialysis bag in phosphate buffer (pH 6.8) to mimic the physiological conditions of the nasal cavity (molecular weight: 12–14 kDa). Dialysis bags were soaked overnight in the dissolution medium. One milliliter each of freshly prepared HupA-NE and Lf-HupA-NE were accurately placed into dialysis bags and tightly sealed. The bags were then placed in 100 mL of release medium and shaken at 37 °C with an agitation speed of 50 rpm. At predetermined time points, 4 mL samples were withdrawn for HPLC analysis, and fresh release medium was added back to the release system. Released HupA-NE and Lf-HupA-NE were compared with the drug suspension under the same sink conditions. The drug contents in each sample were estimated by HPLC. The cumulative percentage of HupA released from the formulations was plotted versus time.

In Vitro Studies

Cell Culture

Human cerebral microvessel endothelial cell/D3 (hCMEC/D3) is an immortalized human BBB cell line that stably maintains a normal BBB phenotype including expression of tight junction proteins, polarized expression of multiple ATP binding cassette (ABC)/solute carrier (SLC) transporters, and restrictive permeability.^{16–18} We hypothesized that NEs interacted with multiple transporters to facilitate passage across the BBB. Endocytosis and transcytosis play key roles in drug delivery to the brain. hCMEC/D3 cells were grown in an incubator with saturated humidity at 37 °C in 5% CO₂ and 95% fresh air. They were maintained in Dulbecco's modified essential medium (1640 from Gibco, Gaithersburg, MD, USA) + 10% fetal bovine serum with 1% penicillin-streptomycin. The cells were trypsinized and split before reaching 90% confluence, typically every 3–4 days. In vitro BBB models were constructed by seeding hCMEC/D3 cells (10⁵ cells/cm²) on the upper side of inserts placed in the wells of 12-well culture plates. (Corning Life Sciences, Corning, NY, USA). Transepithelial electrical resistance (TEER) was recorded 24 h after hCMEC/D3 cells seeding using an epithelial volt/ohm

meter (World Precision Instrument, Sarasota, FL, USA) and was measured for 10 consecutive days.¹⁹

Western Blotting

Western blotting (WB) was performed to determine the expression of P-gp, BCRP, MRP1, and OCT1 in hCMEC/D3 cells. hCMEC/D3 cells were seeded in 12-well plates for 24 h at 37 °C under 5% CO₂. Then, the cells were treated with PBS, HupA-NE, Lf-HupA-NE, or HupA solution (20 μM) for 12 h. Following treatment, the cells were lysed and separated on a 12% sodium dodecyl sulfate-polyacrylamide gels. The proteins were transferred to polyvinylidene membranes, then blocked for 1 h at RT in PBS-Tween (PBS-T) with 5% milk powder, then incubated overnight at 4 °C with primary antibodies against P-gp, BCRP/ABCG2, MRP1, or Oct-1 and gentle shaking. The membranes were then washed three times with PBS-T and incubated for 1 h at RT with goat anti-rabbit IgG (H+L)-horseradish peroxidase, which was used as the secondary antibody. After washing with PBS-T, protein bands were imaged using enhanced chemiluminescence reagents. The membranes were visualized using MicroChem 4.2 (DNR Bio-Imaging Systems, Neve Yamin, Israel).

Transporter Inhibition Assay

hCMEC/D3 cells were seeded (10⁶ cells/cm²) on the apical side of 6-well plates. The cells were grown to 90% confluence. The cells were pre-incubated with different transporter inhibitors and endocytosis inhibitors for 30 min at 37 °C under 5% CO₂. The inhibitors used were as follows: verapamil (10 μM), a P-gp transporter inhibitor; MK571 (10 μM), an MRP1 transporter inhibitor; ko143 (1 μM), a BCRP transporter inhibitor; amantadine (500 mM), an OCT1 transporter Inhibitor; genistein (0.2 M), a caveolae-dependent endocytosis inhibitor; aprotinin (200 μg/mL), a low-density lipoprotein receptor-related protein (LRP) ligand; colchicine (2.5 μM), a pinocytosis inhibitor; and chlorpromazine (10 mg/mL), a clathrin-dependent endocytosis inhibitor. Following pre-incubation, HupA-NE, Lf-HupA-NE, or HupA solution was added to wells containing each inhibitor for 1 h. The wells were washed three times with ice-cold PBS, followed by addition of 1% Triton X-100. The supernatants of the cell lysis solutions were extracted using dichloromethane after centrifugation. Uptake was analyzed by comparing HupA dissolved in methanol by HPLC for each treatment condition.

In Vivo Study

Animals

In vivo studies were carried on adult Wistar rats weighing 200 ± 20 g were purchased from the Experimental Animal Center of Jilin University (Changchun, China). The animals were maintained for two days on a standard diet with free access to water in an air-conditioned room. The room was maintained at 25 ± 1 °C with a relative humidity of $65 \pm 10\%$ and a 12h dark/light cycle (lights on at 7:00 a.m.).

All the animal experiments were conducted according to the National Institutes of Health Guide for the Care and Use of Laboratory Animals (NIH Publications No. 8023, revised 1978), and approved by the Animal Care and Use Committee of the College of Pharmacy of Jilin University (Changchun, China).

Test For Nasal Toxicity Of NEs

Male Wistar rats weighing 200 g were divided into four groups, with three animals in each group. The negative control group received normal saline, the dosage groups received HupA-NE or Lf-HupA-NE, and the positive control group received 1% deoxycholic acid sodium solution in 50 μ L of normal saline intranasally. The rats were given HupA-NE and Lf-HupA-NE for consecutive 14 days. Nasal mucosa was taken on days 1, 7, 14 respectively after rats were sacrificed. The nasal membranes were fixed in 10% buffered formalin for 24 h. The tissues were rinsed under running water, then dehydrated using an ethanol gradient. After dehydration, the tissues were cleared with xylene. The cleared mucosal tissues were immersed in melted paraffin, then cooled prior to slicing. The paraffin sections were stained with hematoxylin and eosin and visualized using an optical microscope.

NE Distribution In The Rat Brain

Animals were anesthetized with diethyl ether, then administered 50 μ L of RhB-HupA solution, RhB-HupA-NE, or Lf-RhB-HupA-NE intranasally (Figure 1). After 1 h, the animals were anesthetized, and their hearts were perfused with saline. The brains were removed, fixed in 4% paraformaldehyde for 48 h, then placed in a 15% sucrose PBS solution for 24 h until subsidence, then in 30% sucrose for 48 h until subsidence. The brains were frozen at -80 °C in optimal cutting temperature embedding medium, then cut into 20 μ m sections using a freezing microtome (Fluorescence Inversion Microscope System, Olympus, Tokyo, Japan). The sections were stained with 300 nM DAPI for 10 min at room temperature, then immediately examined under the fluorescence microscope after washing

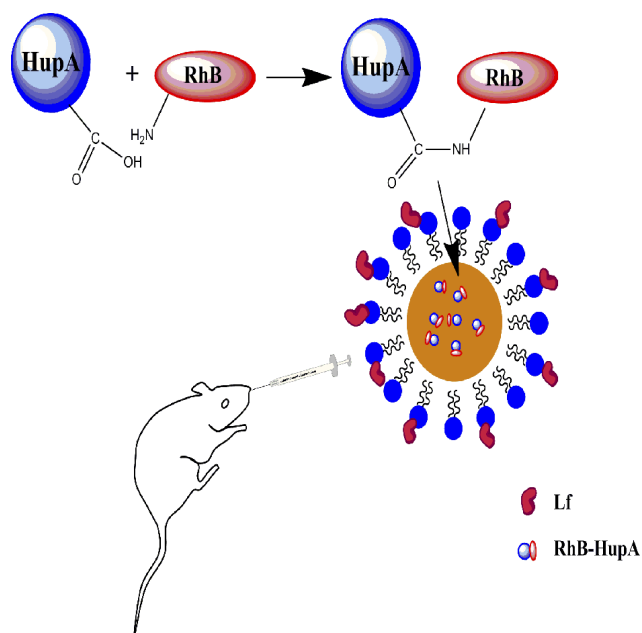


Figure 1 RhB-HupA encapsulated in NE was intranasally administrated to rats.

twice with PBS (pH 7.4). The images were captured using a digital camera (Nikon, Tokyo, Japan).

Pharmacokinetic Study

The rats were anesthetized with a 10% chloral hydrate solution, and 50 μ L of the nasal formulation was administered via a PE 10 tube attached to a syringe inserted 1 cm into the nostril.¹⁰ Orbital blood samples and tissues were collected at 0.083, 0.25, 0.5, 1, 2, 4, 6, 8, 12, 16, and 24 h. Two milliliters of ethyl acetate was added to 2 mol/L NaOH alkalized plasma or tissue homogenates to extract HupA. The ethyl acetate extracts were dried using nitrogen, redissolved in methanol, and analyzed by HPLC. Drug and Statistics 2.0 software program (DAS 2.0, Mathematical Pharmacology Professional Committee of Shanghai, China) was used to calculate the pharmacokinetic parameters. The DTI was calculated to evaluate the brain targeting efficiency. DTI values were calculated as

$$\text{follows: } DTI = \frac{(AUC_{brain}/AUC_{plasma})_{Lf-HupA-NE}}{(AUC_{brain}/AUC_{plasma})_{HupA-NE}}$$

Results

Preparation And Formulation

Optimization Of HupA-Loaded NEs

Solubility Studies

The solubility of HupA in oils, surfactants, and co-surfactants is summarized in Table 1. Cremophor EL was selected as the surfactant due to high HupA solubility

Table 1 Saturation Solubility Of HupA In Different Oils, Surfactants And Co-Surfactants

Vehicles	Compositions	Solubility Of HupA (mg/mL)
Oils		
Soybean oil	Polyoxyethylene castor oil derivatives	2.73±0.07
IPM	Isopropyl myristate	2.43±0.01
L.A.S	Linear Alkylbenzene Sulfonates	34.96±0.13
Capryol90	Propylene glycol monocaprylate	38.33±0.15
LABRAFIL® M 1944 CS	Oleoyl Macroglycerides	19.69±0.24
Grape seed oil	Polyoxyethylene castor oil derivatives	1.96±0.01
Surfactants		
Span 80	Sorbitan Monooleate	13.35±0.12
Cremophor EL	Polyoxyethylene castor oil derivatives	34.70±0.09
Tween 80	Polyoxyethylene-80-Sorbitan Monooleate	21.03±0.45
Plurol® Oleique CC 497	Polyglycerol ester of fatty acids	15.52±0.31
Cosurfactants		
Labrasol	Caprylocaproyl macrogol-8 glycerides	102.21±0.65
PEG400	Polyethylene glycol 400	98.41±0.35
Propanediol	1,2-Propanediol	65.31±0.91

(34.70±0.09 mg/mL). HupA was also highly soluble in Labrasol (102.21±0.65 mg/mL). High drug solubility in the oil phase is important for NE formation, particularly for poorly water-soluble drugs. HupA was most soluble in Capryol 90 (38.33±0.15 mg/mL). IPM has been reported to enhance nasal absorption of drugs,²⁰ so a mixture of IPM and Capryol 90 was chosen as the oil phase. Particle size analysis showed that the mixture of IPM and Capryol 90 produced smaller NEs compared to either oil alone. HupA was also highly soluble in PEG400, but this mixture did not result in transparent NEs.

Pseudo-Ternary Phase Diagram Construction

Phase diagrams were constructed to determine the regions in which NE would form. The pseudo-ternary phase diagrams with different weight ratios of Cremophor EL and Labrasol are displayed in Figure 2. NE formation efficiency was assessed on the basis of the larger NE field in the developed phase diagrams. The NE region reached a maximum at S/CoS of 2:1. As such, a 2:1 ration of Cremophor EL to Labrasol was selected for NE formulation development. The shaded area represents the isotropic and low-viscosity single-phase NE region.

Optimization Of NE Formulation Using BBD Software

A total of 15 experiments were performed to study the effect of formulation variables on globule size and PDI. Response data for all experiments are summarized in

Table 2. Values of “Prob > F” less than 0.0500 indicated significant model terms. Analysis of variance suggested that the Model F values for response size and PDI were 23.07 (p=0.0015) and 26.53 (p=0.0011) respectively, which implied the model was significant.

Adeq precision for response size and PDI were 18.483 and 18.891, respectively. Adeq precision measures the signal to noise ratio, and a ratio greater than 4 is desirable. This model can be used to navigate the design space.²¹ The final equations in term of coded factors for response size and PDI are as follows:

$$\begin{aligned} \text{Size} = & +18.83 + 0.93 * A + 1.91 * B - 1.94 * C - 0.93 * A * B \\ & + 0.10 * A * C - 1.15 * BC + 0.012A^2 + 1.16 * B^2 + 0.052C^2 \end{aligned}$$

$$\begin{aligned} \text{PDI} = & +0.085 - 0.026 * A + 0.033 * B - 0.026 * C - 0.018 * A * B \\ & + 0.012 * A * C - 0.028 * B * C - 0.00096 * A^2 \\ & + 0.036 * B^2 + 0.00097C^2 \end{aligned}$$

The relationship between variables was further studied using three-dimensional (3D) response surface (RS) plots. Figure 3A–C show the effects of factors A, B, and C on response size. RS analysis of size between A and B showed an increasing trend in A and B (Figure 3A). The RS plot for sizes between B and C indicated a non-linear increase in globule size with increased B content and smaller globule size with decreased C content (Figure 3B). Figure 3C shows an increasing trend in size with increased A and decreased C. Hence, to minimize globule size, low levels of A and B and high levels

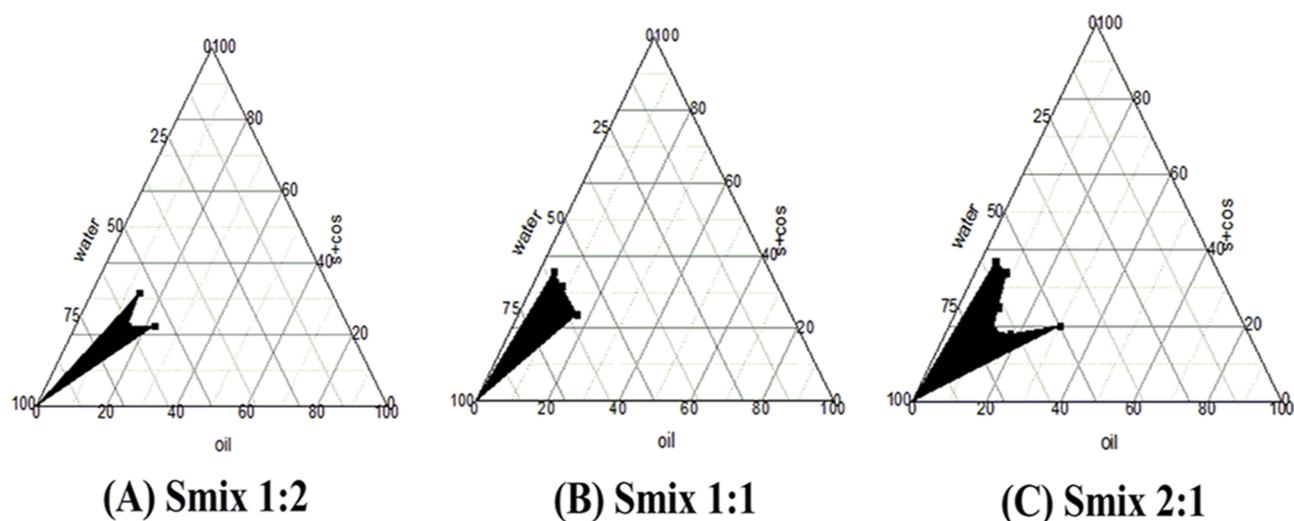


Figure 2 Pseudo-ternary phase diagrams for NE optimization. (A) Smix 1:2, (B) Smix 1:1, and (C) Smix 2:1.

of C were optimal for the final formulation. Similarly, PDI was an important parameter for NE optimization. The RS plot of PDI between A and B showed an increasing trend in PDI with decreased A and increased B (Figure 3D). The RS plot for PDI between A and C (Figure 3E) indicated the decrease in A and increase in C lightly. Figure 3F shows a decreasing trend in PDI with decreased B and increased C. As such, the optimal formulation to reduce the PDI would contain high levels of A and C and low levels of B. Based on these results, the optimized NE with small particle size and low PDI was obtained using concentrations of 3.00% IPM, 3.81% Capryol 90, and 40% S+CoS.

RhB-HupA-NE And Lf-RhB-HupA-NE

The product RhB-HupA was characterized by IR spectra analysis. The spectra of HupA and RhB are shown in Figure 4A and B, respectively. The hydroxyl stretching vibration of carboxylic acid at 2750 cm^{-1} – 3000 cm^{-1} and 1548.73 cm^{-1} of the amino groups had weakened in Figure 4C. Thin-layer chromatography analysis produced a single spot, which demonstrated that RhB was successfully conjugated to HupA.

NE Characterization

Globule Size And Zeta Potential

The average globule sizes of the blank NE, HupA-NE and Lf-HupA-NE were $14.26\pm 0.16\text{ nm}$, $15.24\pm 0.67\text{ nm}$ and

Table 2 Factor Level And Response Data For Full-Factorial Study

Run	Factor 1 A:IPM %	Factor 2 B:Capryol 90%	Factor 3 C:S+CoS%	Response I Size nm	Response I PDI
1	5.00(0)	5.00(0)	35.00(0)	19.00	0.09
2	3.00(-1)	3.00(-1)	35.00(0)	16.91	0.09
3	7.00(+1)	3.00(-1)	35.00(0)	19.82	0.06
4	5.00(0)	3.00(-1)	30.00(-1)	18.63	0.10
5	5.00(0)	7.00(+1)	40.00(+1)	19.16	0.10
6	7.00(+1)	7.00(+1)	35.00(0)	21.25	0.10
7	5.00(0)	3.00(-1)	40.00(+1)	17.09	0.10
8	3.00(-1)	7.00(+1)	35.00(0)	22.04	0.50
9	7.00(+1)	5.00(0)	40.00(+1)	18.36	0.05
10	5.00(0)	5.00(0)	35.00(0)	18.84	0.09
11	5.00(0)	5.00(0)	35.00(0)	18.66	0.08
12	3.00(-1)	5.00(0)	30.00(-1)	19.64	0.14
13	7.00(+1)	5.00(0)	30.00(-1)	22.09	0.08
14	3.00(-1)	5.00(0)	40.00(+1)	15.60	0.07
15	5.00(0)	7.00(+1)	30.00(-1)	25.30	0.21

16.78±0.4nm. (Figure 5A–C) The actual value of NE coincided with the software-predicted value. The zeta potential of the NE was -4.48±0.97 mV (Figure 5D). The zeta potential of HupA-NE and Lf-HupA-NE were -8.06±0.53 and +5.67±0.39 mV (Figure 5E–F).

TEM

TEM analysis confirmed the droplet sizes measured using a Malvern Zetasizer. TEM results for HupA-NE and Lf-HupA-NE are shown in Figure 6.

Stability Study

HupA-NE and Lf-HupA-NE did not exhibit precipitation, creaming, phase separation, or flocculation as determined by visual observation. HupA-NE had a droplet size, PDI, and zeta potential of 16.01±0.75 nm, 0.136±0.018, and -5.23±0.85 mV, respectively. The corresponding values for Lf-HupA-NE were 17.21±0.55 nm, 0.178±0.034, and 4.77±0.96 mV, respectively. Prepared HupA-NE and Lf-HupA-NE were stable for at least 6 months at room temperature.

Drug Release Study

Figure 7 shows the drug release profiles of pure HupA, HupA-NE, and Lf-HupA-NE. Drug release was greater from Lf-HupA-NE than from the pure drug suspension or HupA-NE ($P < 0.001$). The hydrophilicity of Lf allowed contact with the release medium and facilitated release of the drug. Drug release from the HupA solution was faster during the first 4 h compared to that from HupA-NE. As shown in Figure 7, the NE formulations exhibited sustained release. About 85% of drug had released from Lf-HupA-NE at 24 h, compared with 63% release from the pure drug solution at the same time point.

Cellular Studies Of NEs

In Vitro BBB Model

Transwell models were evaluated using TEER for 10 consecutive days. The TEER values increased significantly at the fourth day, reaching 299.04 $\Omega \text{ cm}^2$, suggesting compact cell growth. A liquid level difference >0.5 cm between the upper and lower grids was maintained in the 4h leakage test, demonstrating an obvious barricading effect of the in vitro BBB model.

Expression Of Transporters And Transporter Inhibition Assay

WB results are shown in Figure 8. MRP1 was detected as a single band at 250 kDa. P-gp expression was positive in

hCMEC/D3 cells as a single band at 141 kDa. Previous studies²² reported that Cremophor EL could inhibit P-gp efflux and increase drug absorption. P-gp expression was significantly reduced following treatment with HupA-NE and Lf-HupA-NE. The presence of BCRP was confirmed in hCMEC/D3 cells at 75 kDa. Oct-1 transporter expression levels were below detectable levels in hCMEC/D3 cells. These results showed that hCMEC/D3 cells expressed P-gp, BCRP, and MRP1 transporters.

To study the mechanism of NE transport across the BBB, hCMEC/D3 cells were treated with specific transporter and endocytosis inhibitors prior to incubation. Figure 9A shows that the P-gp inhibitor (verapamil), BCRP inhibitor (ko143), and MRP family inhibitor (MK571) significantly decreased efflux, resulting in increased NE transport into the cells compared to control in hCMEC/D3 cells. The Oct-1 inhibitor amantadine did not significantly affect transport. Figure 9B shows that chlorpromazine (CPZ) and colchicine, both of which inhibit endocytosis, significantly reduced uptake of NEs. Aprotinin restricted transport of HupA-NE across the cells and also mildly reduced Lf-HupA-NE transport. Genistein had the least inhibitory effect.

In Vivo Studies

Test For Nasal Toxicity Of NEs

As shown in Figure 10, none of normal saline (A), HupA-NE (C, E, G) and Lf-HupA-NE (D, F, H) induced nasociliary damage and the epithelial layer was intact. Treatment with 1% deoxycholic acid sodium solution (Figure 10B) caused extensive damage to the nasal mucosa as evidenced by loss of epithelial cells, mucosal layer shrinkage and inflammatory cell infiltration. These results showed that HupA-NE and Lf-HupA-NE were not toxic to the nasal mucosa for 14 days, demonstrating that the excipients used were safe for nasal administration.²³

Qualitative Analysis Of Drug Distribution In The Rat Brain

A preliminary study revealed no fluorescence in non-treated rat brain. (Figure 11A–C) Free RhB-HupA treatment resulted in little signal (Figure 11D–F). Accumulation of RhB-HupA-NE was greater than that of free RhB-HupA in the brain (Figure 11G–I). The greatest accumulation was observed for Lf-RhB-HupA-NE (Figure 11J–L). RhB, which was encapsulated in the nanocarriers as a fluorescent marker, allowed for visualization of HupA distribution in the rat brain.

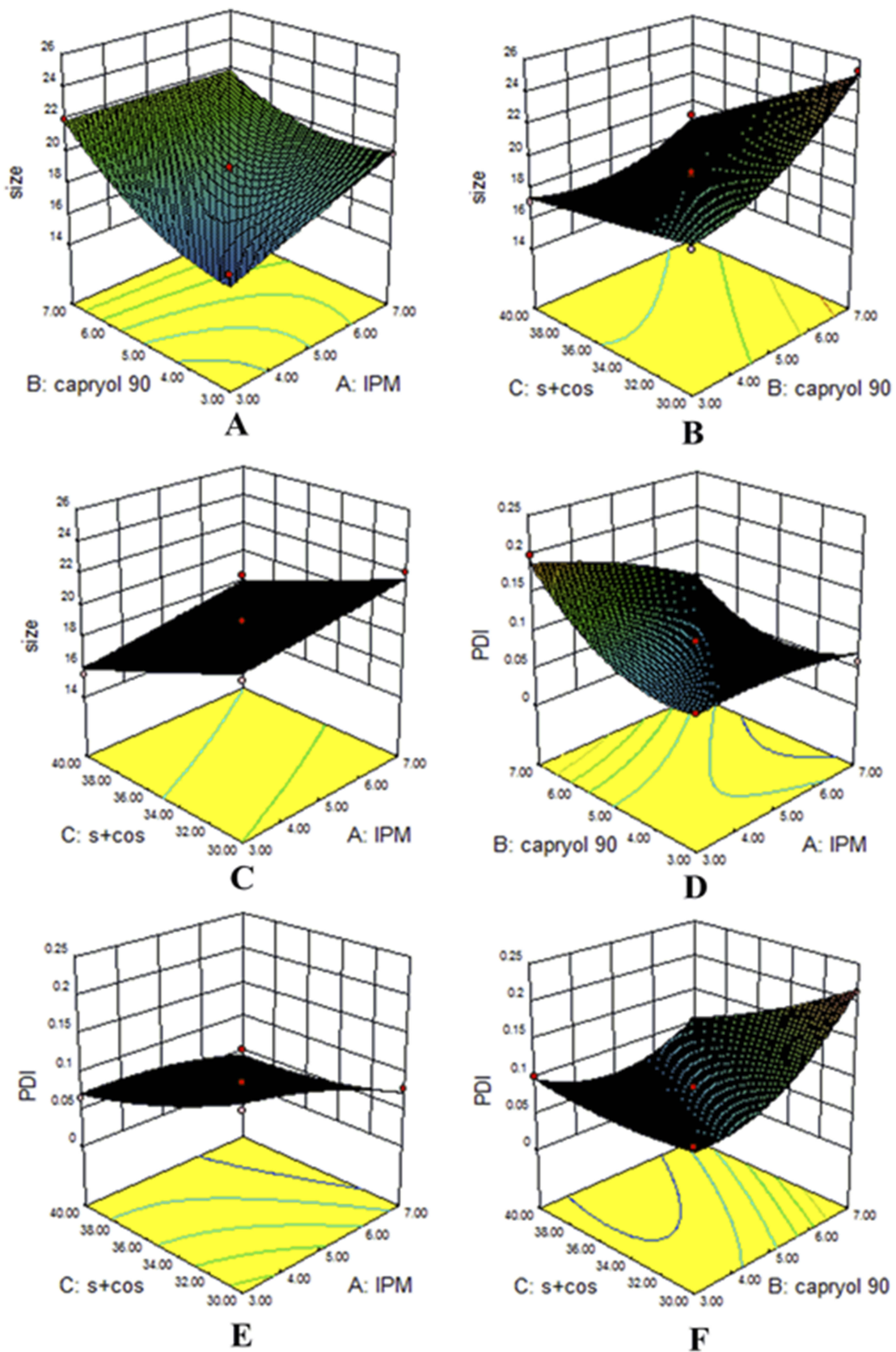


Figure 3 Response surface plots showing significant interaction effects. Globule size (A–C) and PDI (D–F) as the effect of formulation variables.

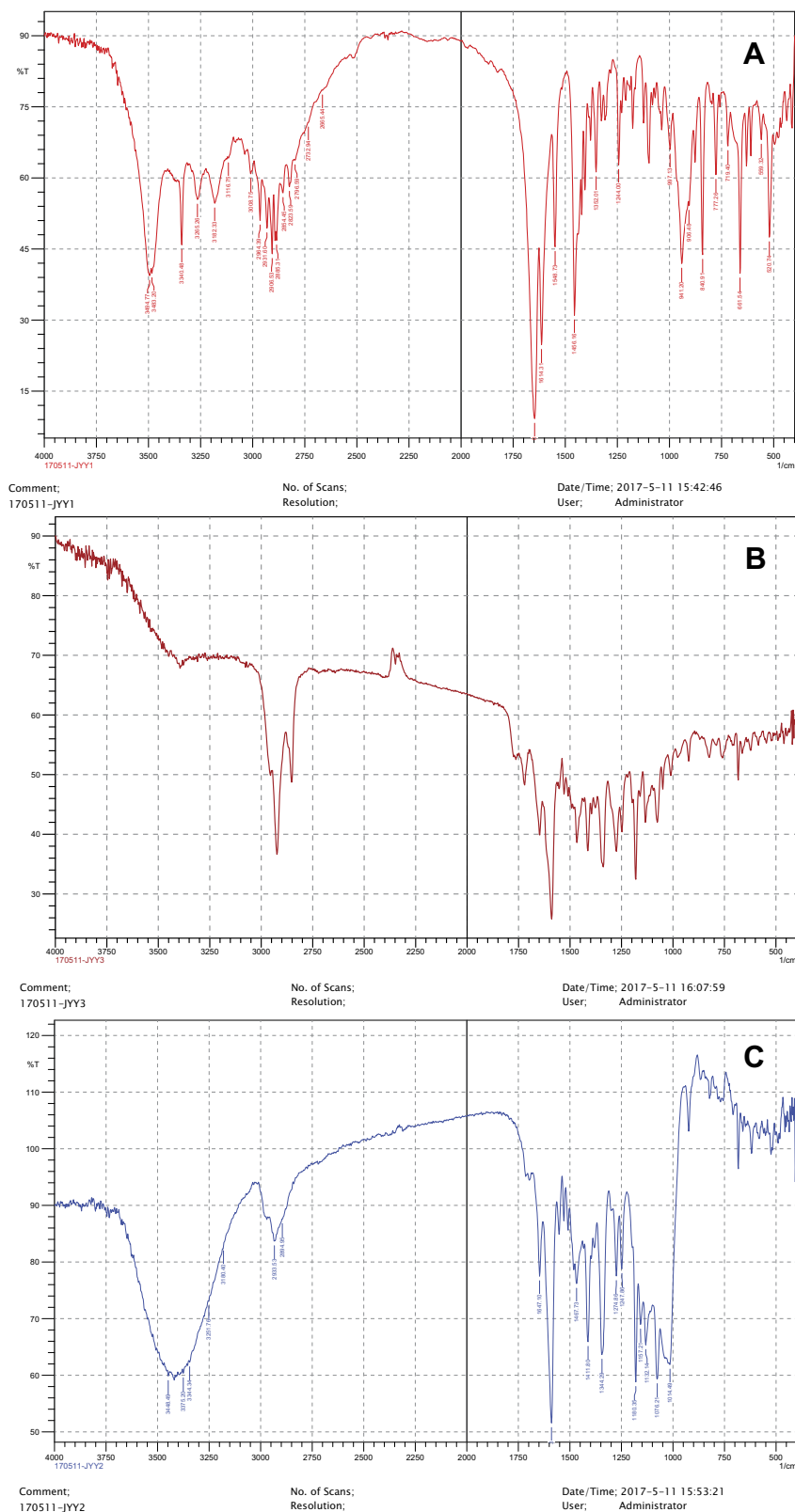


Figure 4 IR spectra for (A) HupA, (B) RhB, and (C) RhB-HupA.

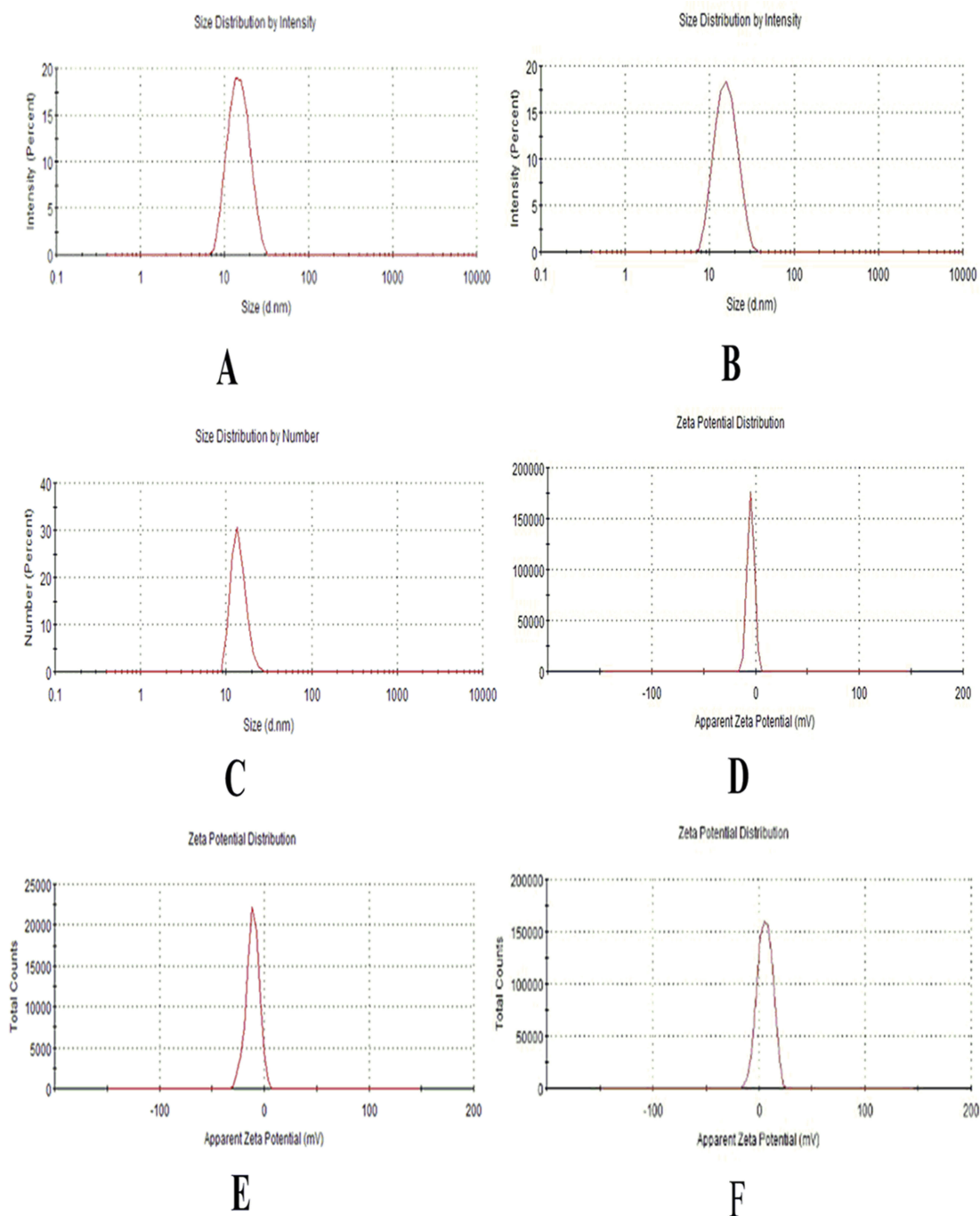


Figure 5 Characterization parameters of optimized NEs (**A–C**) Droplet size distribution of NE, HupA-NE and Lf- HupA-NE, (**D–F**) zeta potential of NE, HupA-NE and Lf- HupA-NE.

Pharmacokinetic Calculations And Statistics

The time course of HupA concentrations in the brain and plasma after intranasal administration of HupA-NE, Lf-HupA-NE, and HupA solution are shown in [Figure 12A](#) and [B](#). There were significant differences among three groups ($p < 0.05$), analyzed by one-way analysis of variance. The pharmacokinetic parameters in the brain and

plasma following intranasal administration are shown in [Tables 3](#) and [4](#).

The concentrations and area under the curves AUC_{brain} and AUC_{plasma} of the NEs were significantly higher than those of free HupA solution at all time points. These results indicated that NEs were more extensively absorbed and transported across the BBB. The AUC_{brain} of Lf-HupA-NE

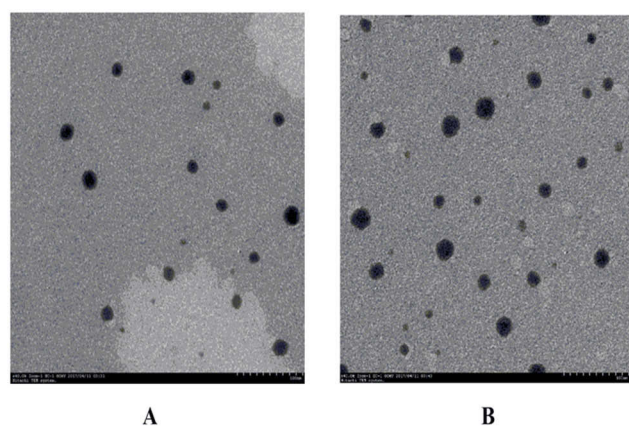


Figure 6 TEM of (A) HupA-NE and (B) Lf-HupA-NE.

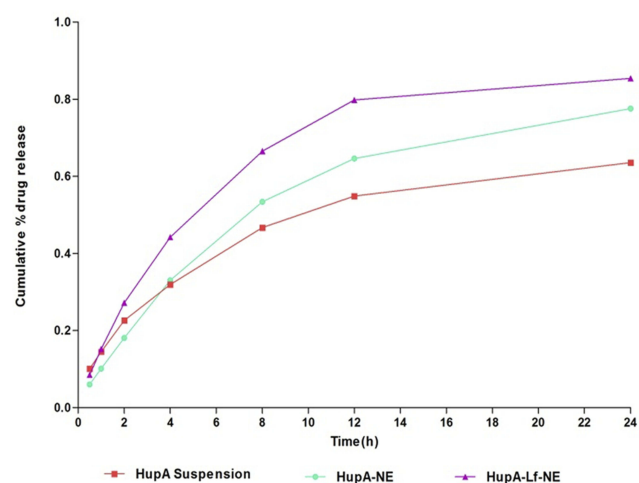


Figure 7 In vitro release results for the HupA suspension, HupA-NE, and HupA-Lf-NE.

was significantly higher than that of HupA-NE, suggesting that the presence of Lf resulted in greater brain uptake. The half-life ($T_{1/2}$) and mean retention time (MRT) of HupA in the brain and plasma were prolonged following treatment with NEs compared with HupA solution. Treatment with the HupA solution resulted in faster metabolism and an earlier peak time than treatment with NEs in the brain. These results indicated that NEs improved absorption and prolonged the duration of action of HupA. The DTI of Lf-HupA-NE in the brain (3.2 ± 0.75) demonstrated effective targeting. These results strongly suggested that Lf-HupA-NE may be a promising nanocarrier to increase nose-to-brain transport.

Discussion

In the present study, we constructed and characterized a novel nano-carrier for intranasal administration. This direct route to the brain²⁴ bypasses gastrointestinal and hepatic

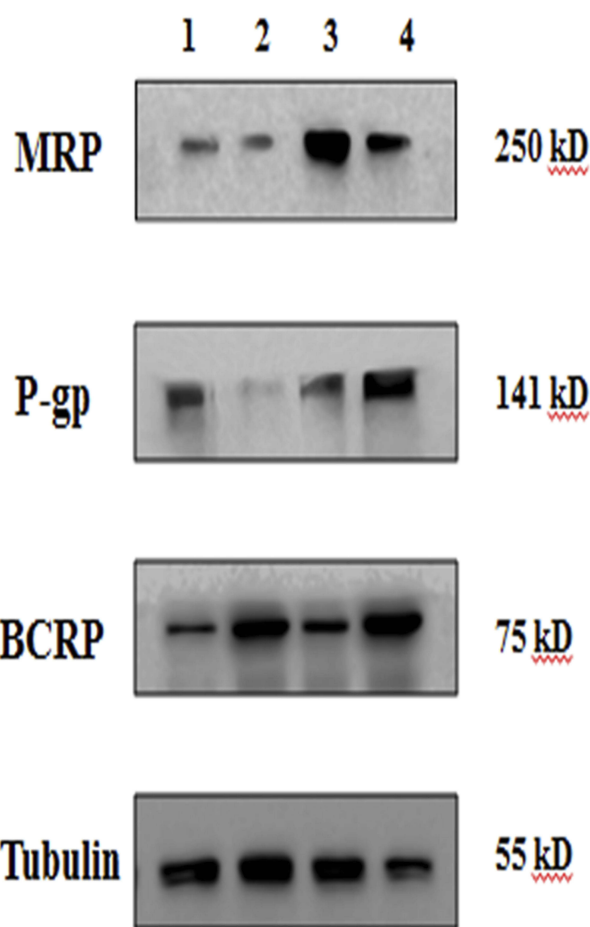


Figure 8 Protein levels of transporters in confluent hCMEC/D3 cells. Lane 1, PBS; Lane 2, HupA-NE; Lane 3, Lf-HupA-NE; and Lane 4, HupA solution.

first-pass metabolism. NEs could increase drug delivery to the brain due to increased solubility and larger surface area. A previous report showed that only nanoparticles with a diameter <20 nm can achieve extracellular transport from the nasal cavity to the brain.²⁵ Whether this occurs through bypassing the BBB or by delivery to the CNS across the BBB is unknown.

NEs composed of oil, surfactants, and co-surfactants should be clear and isotropic at ambient temperature. The choice of excipients is the key factor for NE preparation. Cremophor EL was selected as a surfactant due to its excellent solubilization of HupA. This solubility may have resulted from the ability of the amidogen to form hydrogen bonds with polyethylene oxide (PEO) groups.²⁶ Surfactants lower the interfacial tension to aid the dispersion process and maintain the drug in a solubilized form for effective absorption.^{27,28} Labrasol, which is composed of PEO groups, also solubilized HupA well. Labrasol in combination with Cremophor EL reduced the oil-water interfacial tension,

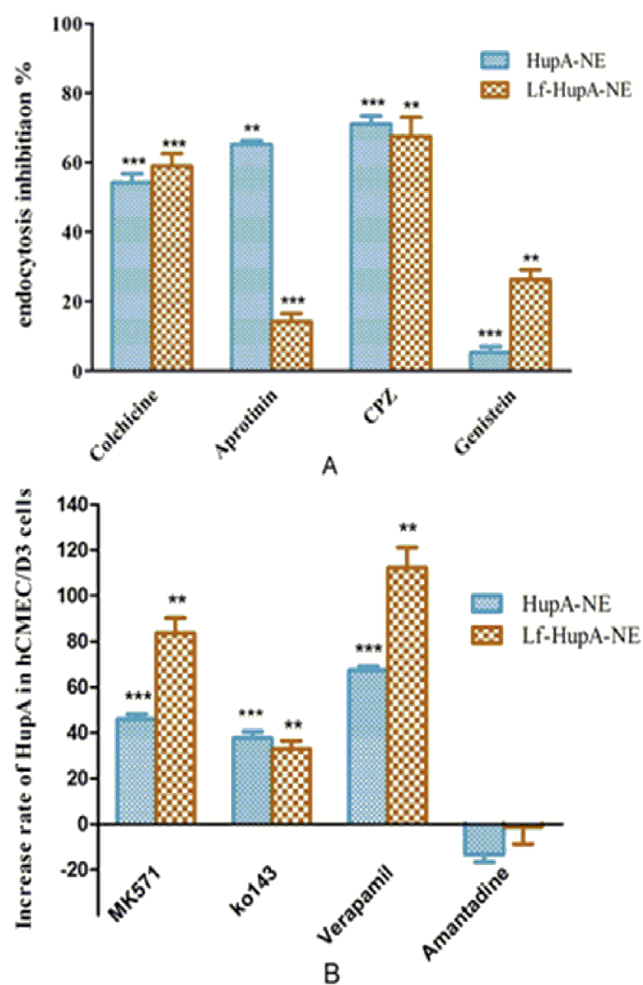


Figure 9 Effects of (A) transporter inhibitors and (B) endocytosis inhibitors on cellular uptake of HupA-NE and Lf-HupA-NE. Values represent the mean \pm SD (n=3). Statistically significant in comparison with normal control **p<0.01, ***p<0.001.

which aided penetration of the hydrophobic region of the oil phase, increased fluidity of the interface of the NE system,²⁹ increased the maximum solubility of HupA and improved drug loading. High drug solubility in the oil phase is important for NE formation, especially for poorly water-soluble drugs. Capryol 90 was chosen as the oil based on its high solubility. This medium chain fatty acid has been widely used in pharmaceutical applications, particularly in NE delivery systems, due to its excellent solubilizing capacity.^{30,31} IPM has been reported to enhance nasal drug absorption.³² As such, a mixture of IPM and Capryol 90 was chosen as the oil phase. Particle size analysis confirmed that the mixture yielded smaller NEs than either oil alone. Ternary-phase studies demonstrated that a 2:1 ratio of Cremophor EL to Labrasol was optimal for NE formulation. Formulation was optimized using BBD as 3.00% IPM, 3.81% Capryol 90, and 40% S+CoS.

Typical NEs have droplet sizes <100 nm, and our results demonstrated that NEs were formed. PDI is a measure of uniformity of droplet size ranging from 0.0 to 1.0. The PDI values of the NEs in this study were closer to 0.0, indicating a concentrated distribution and that the NEs would remain stable. The result of stability study indicated that HupA-NE and Lf-HupA-NE could remain stable for 6 months at room temperature. TEM images showed spherical droplets with no aggregation as dark spots with bright surroundings.

Lf loading of HupA-NE significantly improved drug delivery. Lf is a mammalian cationic iron-binding glycoprotein that binds to Lf receptors. Adsorption of positively-charged NEs to the surface of the negatively charged BBB improves targeting.³³ This paper prepared Lf-HupA-NE with positive charges by screening Lf concentration. The optimum concentration of Lf was 5 mg/mL. Lf-HupA-NE could maintain stable state without any flocculation which was proved by stability study. The Lf receptor (LfR) is expressed on the BBB where it is involved in Lf transport across the BBB in vitro and in vivo through receptor-mediated transcytosis.^{34–36} Li et al used Lf to modify nanoparticle surfaces to improve transport across the BBB via receptor-mediated pathways,³⁷ and Bonaccorso et al demonstrated drug transport directly through nasal tissue to the brain.²⁵

Determining the abilities of HupA-NE and Lf-HupA-NE to cross the BBB required an appropriate in vitro human BBB model. The hCMEC/D3 cell line is an immortalized human BBB cell line that stably maintains a normal BBB phenotype. The morphology closely resembles that of primary cells, forms tight monolayers, has high TEER, and retains important BBB characteristics such as expression of junctional proteins and efflux transporters.³⁸ WB analysis showed that hCMEC/D3 cells expressed multiple transporters including P-gp, BCRP, and MRP1, which are involved in effluxing compounds from the brain capillary endothelial cells into the blood. To explore the mechanism of NE internalization, hCMEC/D3 cells were treated with specific transporter and endocytosis inhibitors. These experiments demonstrated that NE uptake was mediated by specific transporters and endocytosis pathways. CPZ and colchicine inhibit endocytosis and significantly reduced NE uptake. CPZ disrupted clathrin-mediated endocytosis through a mechanism in which adaptor complex 2 (AP2) and clathrin were redistributed away from the plasma membrane, making clathrin unavailable for assembly at the cell surface. Colchicine also inhibits

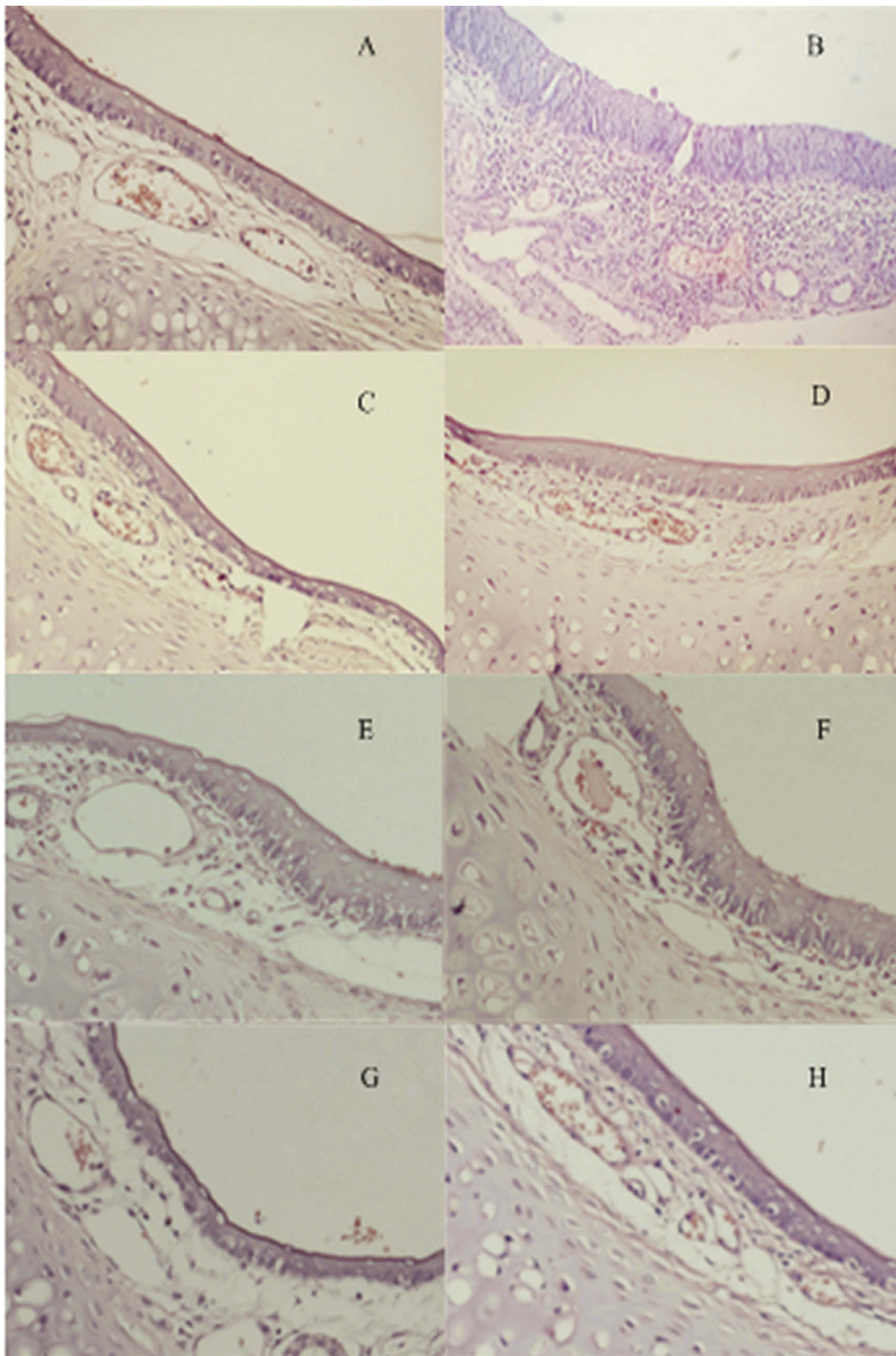


Figure 10 Nasal mucosa of rats treated with (A) normal saline (B) 1% deoxycholic acid sodium solution (C, E, G) HupA-NE on days 1, 7, 14 (D, F, H) Lf-HupA-NE on days 1, 7, 14.

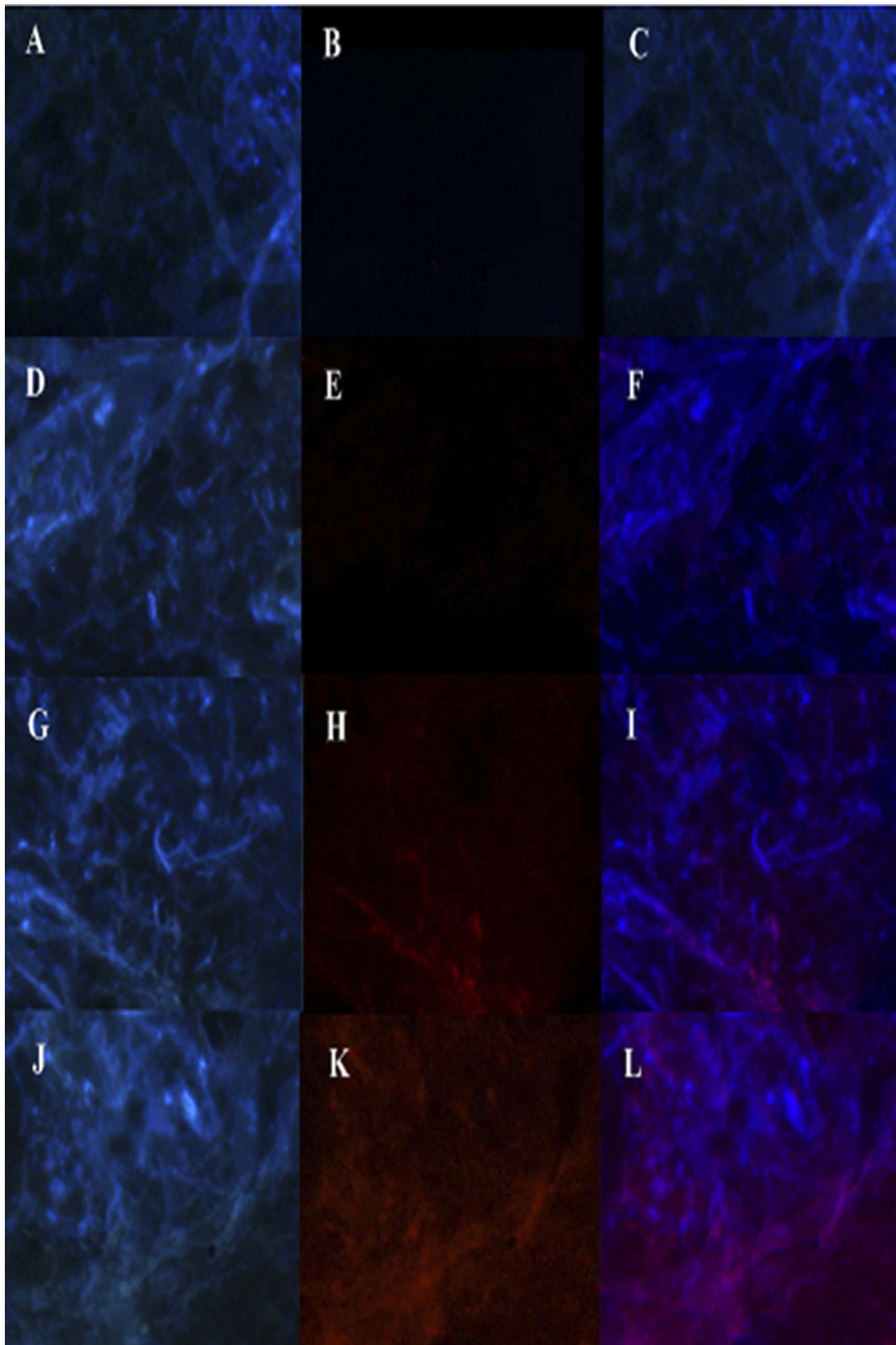


Figure 11 Fluorescence in the brain (A–C) No treatment, (D–F) free RhB-HupA, (G–I) RhB-HupA-NE and (J–L) Lf-RhB-HupA-NE. Red: RhB- HupA, Blue: cell nucleus.

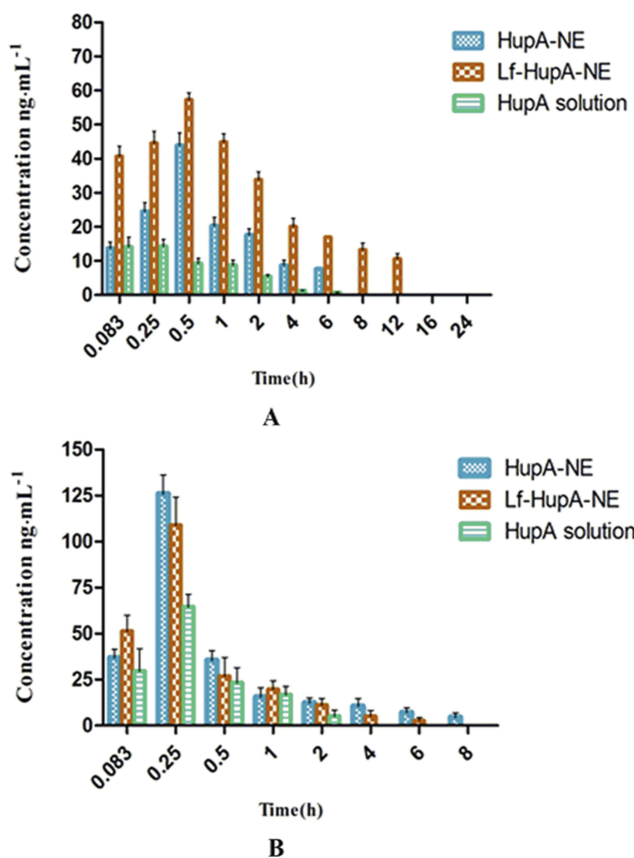


Figure 12 Concentration-time graph of HupA in the (A) brain and (B) plasma after intranasal administration of HupA-NE, Lf-HupA-NE, or HupA solution. Values represent the mean±SD (n=6), p<0.05.

pinocytosis, interferes with microtubule trafficking, and binds to tubulin. Aprotinin binding specificity to LRP receptors decreased unappropriated sites. So the Aprotinin markedly reduced HupA-NE across the cells. Previous studies showed high Lf receptor expression was in respiratory epithelial cells, brain endothelial cells.¹² Lf-HupA-NE can also transport into cells because of its greater affinity for LfR-expressing cells. Therefore, Aprotinin inhibited the transportation of Lf-HupA-NE

Table 3 Pharmacokinetic Parameters Of HupA-NE, Lf- HupA-NE And HupA Solution In The Brain

Pharmacokinetic Parameters	HupA-NE	Lf- HupA-NE	HupA Solution
Cmax (ng/mL)	41.215	58.294	13.29
Tmax (h)	0.5	0.5	0.25
T _{1/2} (h)	3.729	7.128	1.173
AUC(0-t) (ng/mL*h)	86.448	239.643	21.507
AUC(0-∞) (ng/mL*h)	128.206	328.926	23.765
MRT(0-t) (h)	2.178	4.181	1.255
MRT(0-∞) (h)	5.145	9.064	1.674

Table 4 Pharmacokinetic Parameters Of HupA-NE, Lf- HupA-NE And HupA Solution In The Plasma

Pharmacokinetic Parameters	HupA-NE	Lf- HupA-NE	HupA Solution
Cmax (ng/mL)	134.15	105.45	56.95
Tmax (h)	0.25	0.25	0.25
T _{1/2} (h)	7.332	2.884	0.769
AUC(0-t) (ng/mL*h)	101.376	87.755	51.188
AUC(0-∞) (ng/mL*h)	172.519	106.946	51.378
MRT(0-t) (h)	2.451	1.593	1.153
MRT(0-∞) (h)	8.627	3.359	1.439

mildly. Genistein, a caveolin inhibitor, inhibited phosphorylation of the tyrosine. Clathrin-mediated endocytosis and micropinocytosis play important roles mediating NE transport into cells by the LRP receptor.

RhB was used as a fluorescent marker. The conjugation between RhB and HupA was capable of identifying HupA. The fluorescence of RhB-HupA-NE and Lf-RhB-HupA-NE could be utilized to evaluate HupA distribution in the rat brain. The fluorescence intensities of RhB-HupA-NE and Lf-RhB-HupA-NE were higher than that of free RhB-HupA in the rat brain. Furthermore, Lf-RhB-HupA-NE fluorescence was significantly higher than that of RhB-HupA-NE. Lf-HupA-NE had a greater capacity to recognize brain cells because of its greater affinity for LfR-expressing cells. Pharmacokinetics analysis of the different treatments confirmed that NEs improved the absorption and prolonged the duration of action of HupA, particularly Lf-HupA-NE. DTI (3.2±0.75) illustrated that Lf-HupA-NE markedly increased drug delivery to the brain. These results highlighted the superiority of intranasal Lf-HupA-NE for targeting HupA to the brain.

Conclusion

The design of experiment method was successfully used to develop HupA-NE and Lf- HupA-NE. The optimal NE system consisted of Capryol 90, IPM, Cremophor EL, and Labrasol. HupA-NE and Lf-HupA-NE did not exert any toxicity on the nasal mucosa and were stable for 6 months.

hCMEC/D3 cells were used as an in vitro model because they maintain a normal BBB phenotype. NEs interacted with multiple transporters to facilitate passage across the cell monolayer of BBB. Clathrin-mediated endocytosis and micropinocytosis mediated NE transport into cells via the LRP receptor. NEs are transported into the BBB by specific transporters through transcytosis. Our novel brain targeting system Lf-

HupA-NE exhibited a significantly enhanced ability to carry the drug into the brain via intranasal administration without increasing the dose. Lf-HupA-NE was used as a drug carrier to prolong duration of action, target delivery and reduce toxicity. It may be a potential drug delivery system for nose-to-brain delivery. Our findings may have important clinical implications for AD therapy.

Acknowledgments

This work was supported by the Ministry of Science and Technology of Jilin Province, China (201603048YY). We thank Prof. Wei Wu and Dr Liwei Zhao at School of Pharmacy, Fudan University for providing probes.

Disclosure

The authors report no conflicts of interest in this work.

References

- Winblad B, Amouyel P, Andrieu S, et al. Defeating Alzheimer's disease and other dementias: a priority for European science and society. *Lancet Neurol*. 2016;15(5):455–532. doi:10.1016/S1474-4422(16)00062-4
- Fish PV, Steadman D, Bayle ED, Whiting P. New approaches for the treatment of Alzheimer's disease. *Bioorg Med Chem Lett*. 2019;29(2):125–133. doi:10.1016/j.bmcl.2018.11.034
- Wang BS, Wang H, Wei ZH, Song YY, Zhang L, Chen HZ. Efficacy and safety of natural acetylcholinesterase inhibitor huperzine A in the treatment of Alzheimer's disease: an updated meta-analysis. *J Neural Transm*. 2009;116(4):457–465. doi:10.1007/s00702-009-0189-x
- Meng QQ, Wang AP, Hua HC, et al. Intranasal delivery of Huperzine A to the brain using lactoferrin-conjugated N-trimethylated chitosan surface-modified PLGA nanoparticles for treatment of Alzheimer's disease. *Int J Nanomed*. 2018;13:705–718. doi:10.2147/IJN.S151474
- Thomas L, Zakir F, Mirza MA, Anwer MK, Ahmad FJ, Iqbal Z. Development of curcumin loaded chitosan polymer based nanoemulsion gel: in vitro, ex vivo evaluation and in vivo wound healing studies. *Int J Biol Macromol*. 2017;101:569–579. doi:10.1016/j.ijbiomac.2017.03.066
- Anwer MK, Jamil S, Ibnouf EO, Shakeel F. Enhanced antibacterial effects of clove essential oil by nanoemulsion. *J Oleo Sci*. 2014;63(4):347–354. doi:10.5650/jos.ess13213
- Anwer MK, Jamil S, Ibnouf EO, Shakeel F. Enhanced antibacterial effects of clove essential oil by nanoemulsion. *J Oleo Sci*. 2014;63(4):347–354. doi:10.5650/jos.ess13213
- Safari J, Zarnegar Z. Advanced drug delivery systems: nanotechnology of health design A review. *J Saudi Chem Soc*. 2014;18(2):85–99. doi:10.1016/j.jscs.2012.12.009
- Mustafa G, Alrohaimi AH, Bhatnagar A, Baboota S, Ali J, Ahuja A. Brain targeting by intranasal drug delivery (INDD): a combined effect of trans-neural and para-neuronal pathway. *Drug Deliv*. 2016;23(3):933–939. doi:10.3109/10717544.2014.923064
- Zhao Y, Yue P, Tao T, Chen QH. Drug brain distribution following intranasal administration of Huperzine A in situ gel in rats. *Acta Pharmacol Sin*. 2007;28(2):273–278. doi:10.1111/j.1745-7254.2007.00486.x
- Hu KL, Li JW, Shen YH, et al. Lactoferrin-conjugated PEG-PLA nanoparticles with improved brain delivery: in vitro and in vivo evaluations. *J Control Release*. 2009;134(1):55–61. doi:10.1016/j.jconrel.2008.10.016
- Elfinger M, Maucksch C, Rudolph C. Characterization of lactoferrin as a targeting ligand for nonviral gene delivery to airway epithelial cells. *Biomaterials*. 2007;28(23):3448–3455. doi:10.1016/j.biomaterials.2007.04.011
- Qian ZM, Wang Q. Expression of iron transport proteins and excessive iron accumulation in the brain in neurodegenerative disorders. *Brain Res Rev*. 1998;27(3):257–267. doi:10.1016/S0165-0173(98)00012-5
- Mittal D, Md S, Hasan Q, et al. Brain targeted nanoparticulate drug delivery system of rasagiline via intranasal route. *Drug Deliv*. 2016;23(1):130–139. doi:10.3109/10717544.2014.907372
- Ahmad N, Amin S, Neupane YR, Kohli K. Anal fissure nanocarrier of lercanidipine for enhanced transdermal delivery: formulation optimization, ex vivo and in vivo assessment. *Expert Opin Drug Deliv*. 2014;11(4):467–478. doi:10.1517/17425247.2014.876004
- Watson CP, Pazarentzos E, Fidanboyu M, Padilla B, Brown R, Thomas SA. The transporter and permeability interactions of asymmetric dimethylarginine (ADMA) and L-arginine with the human blood brain barrier in vitro. *Brain Res*. 2016;1648:232–242. doi:10.1016/j.brainres.2016.07.026
- Rautio J, Laine K, Gynther M, Savolainen J. Prodrug approaches for CNS delivery. *Aaps J*. 2008;10(1):92–102. doi:10.1208/s12248-008-9009-8
- Sekhar GN, Georgian AR, Sanderson L, et al. Organic cation transporter 1 (OCT1) is involved in pentamidine transport at the human and mouse blood-brain barrier (BBB). *PLoS One*. 2017;12(3):e0173474. doi:10.1371/journal.pone.0173474
- Hatherell K, Couraud PO, Romero IA, Weksler B, Pilkington GJ. Development of a three-dimensional, all-human in vitro model of the blood-brain barrier using mono-, co-, and tri-cultivation transwell models. *J Neurosci Meth*. 2011;199(2):223–229. doi:10.1016/j.jneumeth.2011.05.012
- Richter T, Keipert S. In vitro permeation studies comparing bovine nasal mucosa, porcine cornea and artificial membrane: androstenedione in microemulsions and their components. *Eur J Pharm Biopharm*. 2004;58(1):137–143. doi:10.1016/j.ejpb.2004.03.010
- Sharma N, Singh A, Sharma R. Modelling the WEDM process parameters for cryogenic treated D-2 tool steel by integrated RSM and GA. *Procedia Engineer*. 2014;97:1609–1617. doi:10.1016/j.proeng.2014.12.311
- Shono Y, Nishihara H, Matsuda Y, et al. Modulation of intestinal P-glycoprotein function by cremophor EL and other surfactants by an in vitro diffusion chamber method using the isolated rat intestinal membranes. *J Pharm Sci-U.S.* 2004;93(4):877–885. doi:10.1002/jps.20017
- Sood S, Jain K, Gowthamarajan K. Optimization of curcumin nanoemulsion for intranasal delivery using design of experiment and its toxicity assessment. *Colloid Surface B*. 2014;113:330–337. doi:10.1016/j.colsurfb.2013.09.030
- Mustafa G, Alrohaimi AH, Bhatnagar A, Baboota S, Ali J, Ahuja A. Brain targeting by intranasal drug delivery (INDD): a combined effect of trans-neural and para-neuronal pathway. *Drug Deliv*. 2016;23(3):933–939. doi:10.3109/10717544.2014.923064
- Bonaccorso A, Musumeci T, Serapide MF, Pellitteri R, Uchegbu IF, Puglisi G. Nose to brain delivery in rats: effect of surface charge of rhodamine B labeled nanocarriers on brain subregion localization. *Colloids Surf B Biointerfaces*. 2017;154:297–306. doi:10.1016/j.colsurfb.2017.03.035
- Jaisamut P, Wiwattanawongsa K, Wiwattanapatapee R. A novel self-microemulsifying system for the simultaneous delivery and enhanced oral absorption of curcumin and resveratrol. *Planta Med*. 2017;83(5):461–467. doi:10.1055/s-0042-108734
- Choudhury H, Gorain B, Karmakar S, et al. Improvement of cellular uptake, in vitro antitumor activity and sustained release profile with increased bioavailability from a nanoemulsion platform. *Int J Pharm*. 2014;460(1–2):131–143. doi:10.1016/j.ijpharm.2013.10.055
- Verma S, Singh SK, Verma PRP, Ahsan MN. Formulation by design of felodipine loaded liquid and solid self nanoemulsifying drug delivery systems using Box-Behnken design. *Drug Dev Ind Pharm*. 2014;40(10):1358–1370. doi:10.3109/03639045.2013.819884

29. Bali V, Ali M, Ali J. Novel nanoemulsion for minimizing variations in bioavailability of ezetimibe. *J Drug Target.* 2010;18(7):506–519. doi:10.3109/10611860903548362
30. Pouton CW. Lipid formulations for oral administration of drugs: non-emulsifying, self-emulsifying and 'self-microemulsifying' drug delivery systems. *Eur J Pharm Sci.* 2000;11:S93–S98. doi:10.1016/S0928-0987(00)00167-6
31. Mishra R, Prabhavalkar KS, Bhatt LK. Preparation, optimization, and evaluation of Zaltoprofen-loaded microemulsion and microemulsion-based gel for transdermal delivery. *J Liposome Res.* 2016;26(4):297–306. doi:10.3109/08982104.2015.1120746
32. Richter T, Keipert S. In vitro permeation studies comparing bovine nasal mucosa, porcine cornea and artificial membrane: androstenedione in microemulsions and their components. *Eur J Pharm Biopharm.* 2004;58(1):137–143. doi:10.1016/j.ejpb.2004.03.010
33. Agrawal M, Ajazuddin TDK, Saraf S, et al. Recent advancements in liposomes targeting strategies to cross blood-brain barrier (BBB) for the treatment of Alzheimer's disease. *J Control Release.* 2017;260:61–77. doi:10.1016/j.jconrel.2017.05.019
34. Fillebeen C, Descamps L, Dehouck MP, et al. Receptor-mediated transcytosis of lactoferrin through the blood-brain barrier. *J Biol Chem.* 1999;274(11):7011–7017. doi:10.1074/jbc.274.11.7011
35. Suzuki YA, Lopez V, Lonnerdal B. Mammalian lactoferrin receptors: structure and function. *Cell Mol Life Sci.* 2005;62(22):2560–2575. doi:10.1007/s00018-005-5371-1
36. Huang RQ, Ke WL, Qu YH, Zhu JH, Pei YY, Jiang C. Characterization of lactoferrin receptor in brain endothelial capillary cells and mouse brain. *J Biomed Sci.* 2007;14(1):121–128. doi:10.1007/s11373-006-9121-7
37. Li H, Tong Y, Bai L, et al. Lactoferrin functionalized PEG-PLGA nanoparticles of shikonin for brain targeting therapy of glioma. *Int J Biol Macromol.* 2017;107:204–211.
38. Lukasiewicz S, Blasiak E, Szczepanowicz K, et al. The interaction of clozapine loaded nanocapsules with the hCMEC/D3 cells - In vitro model of blood brain barrier. *Colloids Surf B Biointerfaces.* 2017;159:200–210. doi:10.1016/j.colsurfb.2017.07.053

International Journal of Nanomedicine

Dovepress

Publish your work in this journal

The International Journal of Nanomedicine is an international, peer-reviewed journal focusing on the application of nanotechnology in diagnostics, therapeutics, and drug delivery systems throughout the biomedical field. This journal is indexed on PubMed Central, MedLine, CAS, SciSearch, Current Contents/Clinical Medicine,

Journal Citation Reports/Science Edition, EMBase, Scopus and the Elsevier Bibliographic databases. The manuscript management system is completely online and includes a very quick and fair peer-review system, which is all easy to use. Visit <http://www.dovepress.com/testimonials.php> to read real quotes from published authors.

Submit your manuscript here: <https://www.dovepress.com/international-journal-of-nanomedicine-journal>